Comparison of 16-channel Stripline and 10-channel Fractionated Dipole Transceive Arrays for Body Imaging at 7T

M. Arcan Erturk[1], Alexander J. E. Raaijmakers[2], Gregor Adriany[1], Jinfeng Tian[1], Pierre-Francois van de Moortele[1], Cornelis A. T. van den Berg[2], Dennis W. J. Klomp[2], J. Thomas Vaughan[1], Kamil Ugurbil[1], and Gregory J Metzger[1]

[1]*Center for Magnetic Resonance Research, University of Minnesota, Minneapolis, Minnesota, United States,* [2]*Imaging Division, UMC Utrecht, Utrecht, Netherlands*

Audience. Researchers interested in body/prostate imaging at 7T.

Purpose. MRI of the human torso at 7T is challenging due to destructive interferences resulting in low transmit efficiency and large field inhomogeneities. To address these challenges, it has been demonstrated that multi-channel transmitter coils are needed to optimize transmit B_1 (B_1^+) in the body. Several multi-channel external surface arrays dedicated for 7T MRI body imaging, have been individually characterized and are in use at multiple centers, however the most relevant experimental comparison between these coils using the same scanner do not exist. Here, we experimentally compare transmit and receive performance (B_1^+ performance & signal-to-noise ratio, SNR) of a **16-channel stripline array coil**[1] (**16SA**) and a **10-channel fractionated dipole antenna[2]** (**10DA**) on a deep anatomic target, the prostate, and discuss these results in the context of simulated peak local 10g SAR.

Methods. The **16SA** consisted of a pair of 8 anterior and 8 posterior stripline elements[1]. Briefly, each element had a length of 15 cm, a distance between element centers of 5.5 cm, and were positioned 1.5 cm off the surface of the body with padding. Nearest neighbor elements were capacitively decoupled[1]. All the channels were manually tuned/matched per subject. The **10DA** (MR Coils B.V., Drunen, The Netherlands) consisted of 10 discrete dipole antennae with meanders similar to a previously described 8 channel version[2]. Six elements were placed anteriorly and 4 posteriorly with an 11 cm separation between element centers. The dipole elements were 30cm long and had a fixed distance of 2cm from the subject maintained by the coil's housing. In contrast to 16SA, no additional decoupling circuitry was needed. Axial cross-sections of 16SA and 10DA are shown in **Fig. 1a-b**, respectively.

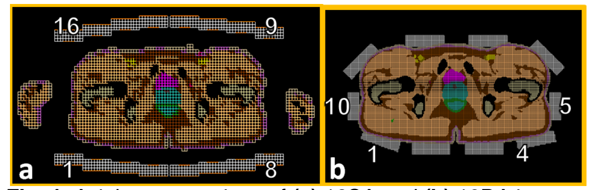

Fig. 1. Axial cross-sections of **(a)** 16SA and **(b)** 10DA in REMCOM software with Duke body model. Coil channels are numbered.

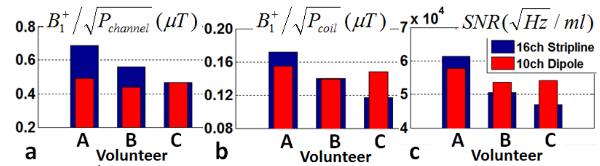

Fig. 2. B_1^+ performance normalized to **(a)** unit power per coil channel, **(b)** total coil power, and **(c)** SNR of 16SA (blue) and 10DA (red) are plotted.

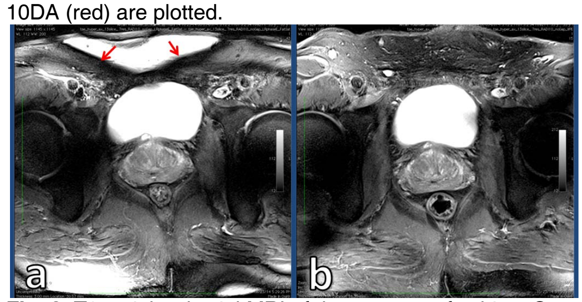

Fig. 3. T2-weighted axial MRI of the prostate of subject C using **(a)** 16SA, and **(b)** 10DA are shown. Red arrows in **(a)** indicate signal inversion.

Safety Evaluation: Local peak 10g-averaged specific absorption rate (SAR) of the coils were computed by electromagnetic (EM) modeling in an anatomically correct model (Duke) using FDTD methods. The 16SA and 10DA were modeled and simulated using Remcom (Remcom Inc., State College, PA) and Semcad X (SPEAG, Zurich, Switzerland), respectively.

Performance Evaluation: MRI experiments were conducted on a Magnetom 7T scanner (Siemens, Erlangen, Germany) equipped with 16 1kW power amplifiers[1]. Transmit phases of the coils were optimized for RF efficiency inside the prostate[3]. A total of 3 subjects (A, B and C) were studied with body mass indices (BMIs) of 21.9, 23.7 and 27.1 corresponding to anterior-posterior (AP) pelvis dimensions of 17.2, 19.0 and 21.4 cm, respectively. SNR data was acquired using a gradient echo sequence (TR/TE=10s/3.1ms, flip-angle=90°, voxel-size=2.7x1.4x3mm^3), followed by a noise scan. Normalized SNR maps were calculated using the methods of Edelstein et al.[4]. B_1^+ maps were calculated from the FA map acquired using the actual flip angle technique[5]. Transmit performance was evaluated in the prostate both in terms of power per channel and per total coil power. Anatomic T2-weighted TSE images were acquired in each subject (TR/TE=6000/72ms, voxel-size= 0.7x0.7x3mm^3, 13 slices).

Results. The performance of 16SA decreased as AP dimension of the subject increased, however the 10DA's performance was more consistent for all body sizes (**Fig. 2**). For subject A (shortest AP distance) 16SA had 6.3% higher SNR and 10.5% higher transmit efficiency than 10DA. However, for subject C (largest AP distance) 10DA performed better in terms of both SNR and transmit efficiency (+15.4% and +26.5%, respectively). B_1^+ per unit power per channel and per total coil power are shown in **Fig. 2a** and **2b**, respectively. Relatively uniform field profile of 10DA was also apparent in T2w images of subject C (BMI 27.1); the 16SA image (**Fig. 3a**) showed a signal inversion band on the anterior side of the bladder whereas the 10DA image (**Fig. 3b**) did not. 10g peak local SAR per unit power per element (SAR/W) was 8.3 and 4.3W/kg for 16SA and 10DA, respectively.

Discussion / Conclusion. This comparison is of existing realizations of two actively used transceiver array concepts. For targets closer to the coil and/or in smaller subjects, 16SA can perform better than 10DA for a given input power per element. For larger subjects and deeper targets, 10DA is more advantageous, and it can provide a more uniform field profile across the torso. There is a crossover point at BMIs of ~26-27 for transmit and receive performance, respectively, where the 10DA begins to perform better than the 16SA[6]. It should be mentioned that the average BMI in the EU and the US are ~26.5 and 28.6, respectively. EM simulations show that each element of 10DA can receive 1.9-fold more power per element than the 16SA while not exceeding local 10g average SAR. Therefore, if not limited by peak RF power and using the metric of B_1^+ normalized by SAR, the B_1^+ of the 10DA would outperform the 16SA in nearly all situations. *Practical Considerations:* Advantages of the 16SA are that it is easier to position on unique body geometries because of the shorter elements and currently can accommodate more padding posteriorly. Advantages of the 10DA are that it has a low Q and does not require subject dependent tuning and matching of each element.

References. **[1]** Snyder (2012) MRM 67:954-964. **[2]** Raaijmakers (2014) ISMRM p314. **[3]** Metzger (2008) MRM 69:396-409. **[4]** Edelstein (1986) MRM 3:604-618. **[5]** Yarnykh (2007) MRM 57:192-200. **[6]** Raaijmakers (2014) ISMRM p4887.

Acknowledgements. Supported by: NCI R01 CA155268, WM Keck Foundation, NIH S10 RR026783, NIBIB P41 EB015894.